ESD-TR-69-320

Technical Note 1969-53

R. K. Crane

Predictions of Transhorizon Field Strengths Using Modeling Techniques

17 October 1969

Prepared under Electronic Systems Division Contract AF 19(628)-5167 by

Lincoln Laboratory
MASSACHUSETTS INSTITUTE OF TECHNOLOGY
Lexington, Massachusetts

MASSACHUSETTS INSTITUTE OF TECHNOLOGY

LINCOLN LABORATORY

PREDICTIONS OF TRANSHORIZON FIELD STRENGTHS USING MODELING TECHNIQUES

R. K. CRANE

Group 61

TECHNICAL NOTE 1969-53

17 OCTOBER 1969

LEXINGTON MASSACHUSETTS

The work reported in this document was performed at Lincoln Laboratory, a center for research operated by Massachusetts Institute of Technology, with the support of the Department of the Air Force .under Contract AF 19(628)-5167.

ABSTRACT

Four propagation mechanisms are known which can cause detectable signal levels beyond the horizon. To investigate the potential of these mechanisms for causing interference, typical and extreme values were computed for models of the different propagation mechanisms, terrain diffraction, turbulent scattering, precipitation scattering, and ducting. The propagation path used for the model computations was 175 km long passing over irregular low lying terrain. The terminals of the path were taken to model a possible satellite earth station, radio relay station configuration. The radio relay station was assumed to have an antenna with a 2.5° half-power beamwidth pointing at an elevation angle of 0.5° to the horizon. The earth station antenna was assumed to have a 0.5° half-power beamwidth. A wavelength of 5 cm was used for the computations. Using the CCIR recommendations as a standard for interference levels, a propagation loss of less than 91 db relative to free space will cause interference for this path.

The highest signal strengths for this path were caused by turbulent scattering, precipitation scattering, and ducting. For both antennas elevated 0.5° to the horizon and pointed along the great circle route values of loss relative to free space of 50 db were computed for an extremely strong turbulent layer, 70 db for a typical turbulent layer and 58 db for a typical thundershower. For

each of these computations the layer or storm was placed in the center of the common volume. For the antennas elevated to the same angle but each pointed approximately 7° off axis the extreme layer and the storm would cause interference, the computed loss for each being 80 and 58 db, respectively. For both antennas pointed along the great circle path and the earth station antenna at 5.0 elevation angle, precipitation scattering would cause interference with a loss of 69 db. For ducting and both antennas pointed along the great circle path and at elevations below 0.5, fields in excess of free space are possible.

The model computations show that for a spacing of 175 km, with low lying intervening terrain, and with the earth station antenna elevated above 5° precipitation scattering and ducting will be the only sources of interference. The problem of ducting can be reduced by siting so that shielding hills surround the earth station keeping the minimum elevation angle above 0.5.

Accepted for the Air Force
Franklin C. Hudson
Chief, Lincoln Laboratory Office

Predictions of Transhorizon Field Strengths Using Modeling Techniques

This study resulted from a request by the Assistant Director, Communications and Electronics, Office of the Director of Defense Research and Engineering of the Department of Defense to explain some of the results of the POPSI measurement program (Carey et al, 1968). The results of the study were presented to the Office of Telecommunications Management in 1967 and presented at the Fall 1967 NEREM Meeting. This report has been prepared to meet the continuing demand for information on the subject.

A. The Use of Models

The estimation of interference level signal strengths at one location on the ground due to a source at another location requires a knowledge of the transmission loss between the two locations. The transmission loss depends upon the terrain, the antennas used at each location, and the structure of the atmosphere between the two locations. For the same terrain and antenna configuration the transmission loss may vary widely from day to day. The statistics of the loss depend upon the statistics of the atmospheric structure. The connection between a description of atmospheric structure and transmission loss is difficult to make and at any particular time the structure is not known well enough for detailed computations of the transmission loss. Model computations can, however, be made that relate gross features of the atmospheric structure to ranges of possible values of the transmission loss.

The current requirement for transmission loss prediction is to estimate the signal strength that would occur on the average for four minutes of the worst month or 0.01 percent of the time. An empirical determination of the expected transmission loss that is exceeded only four minutes per month would take many years. This problem is, however, easily handled by the modeling method because all that is required is the estimation of the lowest possible transmission loss consistent with possible atmospheric structures.

The application of modeling techniques presupposes a knowledge of the mechanisms that cause transhorizon fields. Using our current knowledge of atmospheric structure, four mechanisms can be identified, terrain diffraction, turbulent scattering, precipitation scattering, and ducting. On a particular transmission path one or all of the above mechanisms may be important.

B. Terrain Diffraction

For paths where edges of terrain features such as mountains or hills are simultaneously visible (line-of-sight at the frequency of interest) from both locations, terrain diffraction is a possible source of interfering level signals. Methods useful for estimating the signal levels at the frequencies of interest are available in the literature (Rice, et al, 1965; Deygout, 1966) and have been checked experimentally (Carlson and Waterman, 1966). For long-distance paths over low lying irregular terrain multiple terrain diffraction will occur and the resultant signal strength is negligible compared with that caused by other mechanisms.

C. Turbulent Scattering

The term-turbulent scattering, or better perhaps scattering due to refractive index fluctuations, is applied to all random atmospheric structures which cause scattering (Tatarski, 1961). This technique applies equally well to scattering due to "volume turbulence" and to "feuillets" as described by DuCastel (1966). Using this technique, the bistatic scattering cross section per unit volume is related to the spatial three-dimensional power spectrum of the departure of the index refraction from a mean value.

$$\beta_{\perp}(\vartheta) = 8\pi^2 k^4 \tilde{\Phi}_n(\underset{\sim}{k} - k\hat{m})$$

$$\beta_{||}(\vartheta) = \beta_{\perp}(\vartheta) \cos^2\vartheta$$

where

$\beta_{\perp}(\vartheta)$ = bistatic scattering cross section per unit volume for polarization perpendicular to the plane of scattering.

$\beta_{||}(\vartheta)$ = bistatic scattering cross section per unit volume for polarization parallel to the plane of scattering.

ϑ = scattering angle.

k = $2\pi/\lambda$ = wave number.

$\underset{\sim}{k}$ = vector pointing in the direction of propagation with a magnitude equal to k.

$\hat{m}$ = unit vector pointing from scatterer to receiver.

$\tilde{\Phi}_n(\underset{\sim}{x})$ = spatial power spectrum of refractive index in homogenetic.

For a turbulent medium and wave numbers in the inertial subrange, the spatial power spectrum is given by the "minus 11/3-power law" and the bistatic scattering cross section is given by

$$\beta_{\perp}(\vartheta) = 8\pi^2 k^4 \left[0.033\, C_n^2 \left(2k \sin\frac{\vartheta}{2}\right)^{-11/3} \right]$$

$$= \frac{1.757\, C_n^2}{\lambda^{1/3}} \left(\sin\frac{\vartheta}{2}\right)^{-11/3}$$

λ = wavelength in cm

C_n^2 = value related to the strength of refractive index fluctuations in the atmosphere with units of $m^{-2/3}$.

$$1 \text{ cm} < \frac{\lambda}{4\pi \sin\left(\frac{\vartheta}{2}\right)} < 10^3 \text{ cm} \quad .$$

The atmosphere is typically turbulent and for modeling purposes and for frequencies in the range of interest (1 to 40 GHz) the scattering cross section for the inertial subrange is used.

To model atmosphere effects, the value of C_n^2 must be known. A profile of C_n^2 showing an extreme layer is given in Fig. 1. This profile was generated from a RAWIN sounding using the techniques of Vasil'chenko (1966) to estimate the turbulence coefficient and the methods of Tatarski to relate this to C_n^2.

Verification of the general shape of the profile has been provided by Hardy, et al (1966), Lane (1967), and Crane (1968).

The estimation of signal strength requires the estimation of the volume of space having the bistatic scattering cross section defined above. From the profile, the occurrence of thin layers is noted. For a model, an extreme layer can be taken as having a thickness of 100 meters and a strength of $C_n^2 = 10^{-13}\ m^{-2/3}$. The volume contributing to the scattered signal is given by the common occurrence in space of the two antenna beams and the layer. The transmission loss relative to free-space loss is given by

$$L = \frac{4\pi r_1^2 r_2^2}{d^2 \beta_\perp(\vartheta) V} \tag{1}$$

V = volume of scatterers defined by the layer and the antenna patterns.

r_1 = distance from source to scatterer.

r_2 = distance from receiver to scatterer.

d = distance from source to receiver.

For the case where both antennas are pointed at the same spot on the layer

$$\frac{P_r}{P_t} = \frac{G_1 \eta_2 A_2 V \beta_\perp}{(4\pi)^2 r_1^2 r_2^2} \tag{2}$$

$$= \frac{1.1\, A_s \eta_\ell \eta_s (\psi_\ell + \psi_s)^{-11/3}}{d_s^2 \lambda^{1/3} \qquad \psi_\ell} (\Delta h\, C_n^2) \tag{3}$$

where

A_s = area of the smaller aperture in m.

η_ℓ, η_s = efficiency of the larger (ℓ) and smaller (s) apertures

d_s = distance to the spot on the layer from the smaller aperture

Δh = thickness of layer in m.

G_1 = gain of transmitter

η_2 = efficiency of receiver

A_2 = area of receiver aperture

P_t = transmitter power

P_r = received power

ψ_ℓ = angle between ray from large aperture to spot on layer and the intersection of the layer and the scattering plane (plane including spot, transmitter, and receiver)

ψ_s = angle defined as for ψ_ℓ except using the ray from the smaller aperture

D. Precipitation Scattering

The term precipitation scattering refers to scattering by particulate matter in the atmosphere. For the frequency range of interest the precipitation particles, rain, snow, hail and sleet cause the scattered fields. For rain, the bistatic scattering cross section per unit volume can be related to the backscatter cross section per unit volume for the frequencies of interest (Crane, 1966).

$$\beta_{\perp}(\vartheta) = \beta_{back} = \frac{Z_{eff}\pi^5 |K|^2}{\lambda^4} \tag{4}$$

$$\beta_{||}(\vartheta) = \cos^2\vartheta \ \beta \ (\vartheta)$$

where Z_{eff} is the frequency normalized backscatter cross section used to describe rain by radar meteorologists.

$|K|^2 = 1$ a parameter depending upon the dielectric constant of water. For precipitation particles other than rain, a more complicated angular dependence is found (Dennis, 1961). The extreme values of the scattered field orginate in the cores of thunderstorms. There the particulate content is rain and hail. The properties of hail may be estimated to first order in the same manner as for rain.

The basic data required to make estimates of the precipitation scattered field strength is that provided by the weather radars. Extreme values of $Z = 10^6 \ mm^6/m^3$ have been measured that apply to cores roughly 5 km in diameter and extending from the surface to a 15 km height. An example of a rain-cell core of this size is given on the maps in Fig. 2 as an area labeled as 4. For this extreme model, the scattering volume is limited by the common occurrence of the rain and the antenna beams. For many problems, the occurrence of rain, one main beam, and the side lobes from the other antenna must be considered (Altman, 1967). The transmission loss is given by Eqs. (1) and (4) where the volume is defined by the antenna patterns and the precipitation particles.

E. Ducting

Ducting describes the mechanism for directing energy from one location to another by bending the direction of propagation such that the energy propagates along thin layers in the atmosphere or in a surface layer touching the ground. The prediction of signal strength due to ducting for given atmospheric structures is very difficult unless the structure conforms to the simple models for which mathematical computations are valid. As an extreme model zero db loss relative to free space may be assumed for locations near or over water as has been reported from measurements (Kerr, 1951). The application to overland locations is far more difficult.

F. The Application of Modeling Techniques to a Sample Path

Data from the POPSI experiment conducted by the FCC* for the Highlands to Wildwood, New Jersey path for the week of 2-9 August 1966 was provided for comparison with model predictions. The geometry for the great circle path is given in Fig. 3. The data received for three different transmitter pointing angles are given in Figs. 4 to 6. The CCIR interference level was

---

* Courtesy of R. B. Carey, Research Division, FCC.

chosen to provide a minimum path loss $(\frac{P_r}{P_t})$ of 244 db or a loss relative to free space of 91 db. This differs from the criterion used by the FCC in analyzing the POPSI data. For this path the terrain was low lying, the distance long and terrain diffraction effects can be ignored. The other mechanisms have unique fading patterns as shown in Figs. 7 to 9 and the occurrence of each mechanism could be tabulated using the measured data. For the samples used to generate the cumulative distributions, the percent time of occurrence of each mechanism is indicated by bars along the lower edge of the figures. In a few cases some uncertainty as to mechanisms, ducting or turbulent scatter, was present and classification was made using the depth of the fading, fades greater than 15 db were attributed to ducting.

The data for the "calibration path" was replotted for each mechanism separately as shown in Figs. 10 to 12. The data for turbulent scattering follows a log normal distribution which, using a criterion often used by communications engineers, indicates a common mechanism. The data for ducting with the on-path receiver similarly shows the same log normal behavior. The off-path data does not. For several sample times the off-path receiver had signal strengths equal to, or greater than, the on-path receiver. It is felt that this is due to terrain scattering within the duct but further analysis must be made of this point. The data for rain cannot be classified by the shape of the cumulative distribution but this is expected since the sample size is extremely small.

For the path, the geometry for turbulent scattering layers is shown in Fig. 13. The following extreme signal predictions are made using the model above where L is loss relative to free space.

L_1 = 50 db for the optimally positioned layer, both antennas at 0.5° elevation and pointed along the great circle path.

L_2 = 80 db for both antennas at 2°, the receiver 6° off axis and the transmitter 9° off axis.

L_3 = 96 for both antennas pointed along the great circle path, the receiver at 5° and the transmitter at 0.5 elevation angle.

The extreme value for L_1 estimated from the data gives 48 db for 0.01 percent of the time by extrapolating along the straight line. The data for L_2 and L_3 are inconclusive due to the limited amount of data, the limited dynamic range of the system, and the curves not being separated by mechanisms.

The model computations for precipitation used the geometry of Fig. 14 and the backscatter cross section and rain volume specified above and the transmitter and receiver pointing angles specified above are:

L_1 = 58 db

L_2 = 58 db

L_3 = 69 db .

These results are difficult to compare with the measurements because of the lack of rain.

The estimated extreme values for ducting are taken from the sum of the difference between the antenna main lobe gain and the side-lobe gain at the angle for optimum coupling into the duct for each antenna. These numbers are:

$$L_1 = 3 \text{ db}$$

$$L_2 = 50 \text{ db}$$

$$L_3 = 27 \text{ db} \quad .$$

These estimates compare favorably with the estimates taken from the measured data by extrapolating along the "best fit" line.

The results of the estimates of extreme values agree reasonably well with the extrapolated results of the measured data providing enough data points are taken. The results on rain are inconclusive and a more detailed computation using an entire rain storm for a model not just a rain cell is required. The turbulent scatter data is inconclusive for other than the calibration path.* To get a better estimation, the results must be obtained using the full antenna patterns and the extreme layer model. This is evident from the data because for the elevated transmitter case, 8 of the 24 measurements made during conditions of turbulent scatter produced measurable results.

---

* A better check on this model is provided by Crane (1968).

REFERENCES

P. L. Rice, A. G. Longley, K. A. Norton and A. P. Barsis, "Transmission Loss Predictions for Tropospheric Communication Circuits," NBS Technical Note, 1 and 2, No. 101 (May 1965).

J. Deygout, "Multiple Knife-Edge Diffraction of Microwaves," IEEE Trans. Antennas Propag. AP-14, No. 4, 480-489 (1966).

A. B. Carlson and A. J. Waterman, Jr., "Microwave Propagation Over Mountain-Diffraction Paths," IEEE Trans. Antennas Propag. AP-14, No. 4, 489-496 (1966).

V. I. Tatarski, Wave Propagation in a Turbulent Medium (McGraw-Hill Book Co., New York, 1961).

F. DuCastel, Tropospheric Radiowave Propagation Beyond the Horizon, (Pergamon Press, Oxford, 1966).

V. I. Vasil'chenko, "Relationship Between the Turbulence Coefficient and the Vertical Distribution of Temperature and Winds in the Lower 300-M Layer as Indicated by Ballon Data," Trudy Glavnoy Geofizicheskoy Observatorii," No. 185, 68-81 (1966).

K. R. Hardy, D. Atlas and K. M. Glover, "Multiwavelength Backscatter from The Clear Atmosphere," J. Geophys. Res. 71, No. 6, 1537-1552 (1966).

J. A. Lane, "Radar Echoes from Tropospheric Layers by Incoherent Back Scatter," Electronics Letters, 3, No. 4, 173-174 (1967).

R. K. Crane, "Microwave Scattering Parameters for New England Rain," Technical Report 426, Lincoln Laboratory, M. I. T. (October 1966), DDC AD-647798.

A. S. Dennis, "Forward Scatter from Precipitation as an Interference Source at Stations Monitoring Satellites," Stanford Research Institute, SRI Project 3773, Research Memo 2 (Revised) (November 1961).

F. J. Altman, "Precipitation Scatter Interference Between Space and Terrestial Communication Systems," Communication Systems, Inc., Report No. 453340 (October 1967).

D. E. Kerr, Propagation of Short Radio Waves, M. I. T. Radiation Laboratory Series, 13 (McGraw-Hill Book Co., New York, 1951).

R. K. Crane, "Monostatic and Bistatic Scattering from Thin Turbulent Layers in the Atmosphere," Technical Note 1968-34, M. I. T. Lincoln Laboratory (18 September 1968), DDC AD-678061.

R. B. Carey, D. B. Hutton and G. S. Kalagian, FCC/USAF POPSI Project, Report R-6801, Federal Communications Commission Research Division (March 5, 1968).

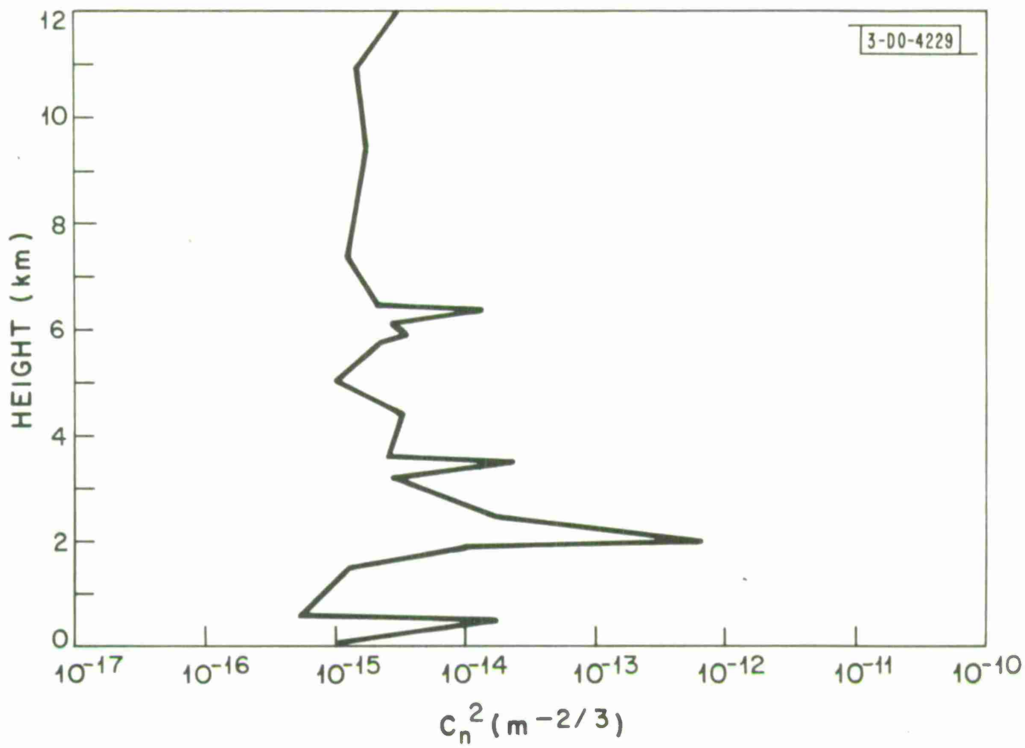

C_n^2 PROFILE COMPUTED FROM RAWINSONDE DATA (GMD^{-1})
3 AUG 66 0600 GMT
WALLOPS ISLAND STATION

Fig. 1.

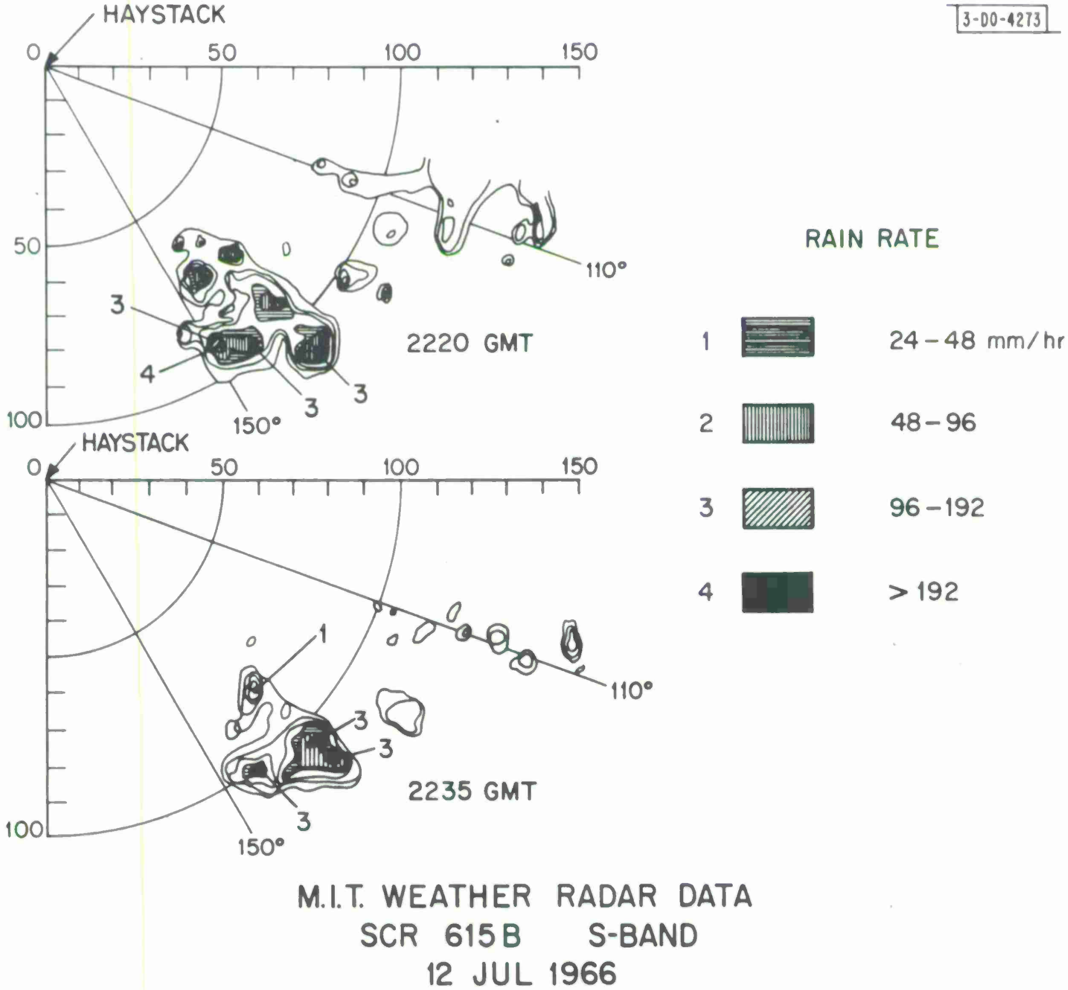

3-D0-4273
HAYSTACK
0
50
100
150
50
100
110°
150°
3
4
3
3
2220 GMT
HAYSTACK
0
50
100
150
100
110°
150°
1
3
3
3
2235 GMT
RAIN RATE
1
24 – 48 mm/hr
2
48 – 96
3
96 – 192
4
> 192
M.I.T. WEATHER RADAR DATA
SCR 615B S-BAND
12 JUL 1966

Fig. 2.

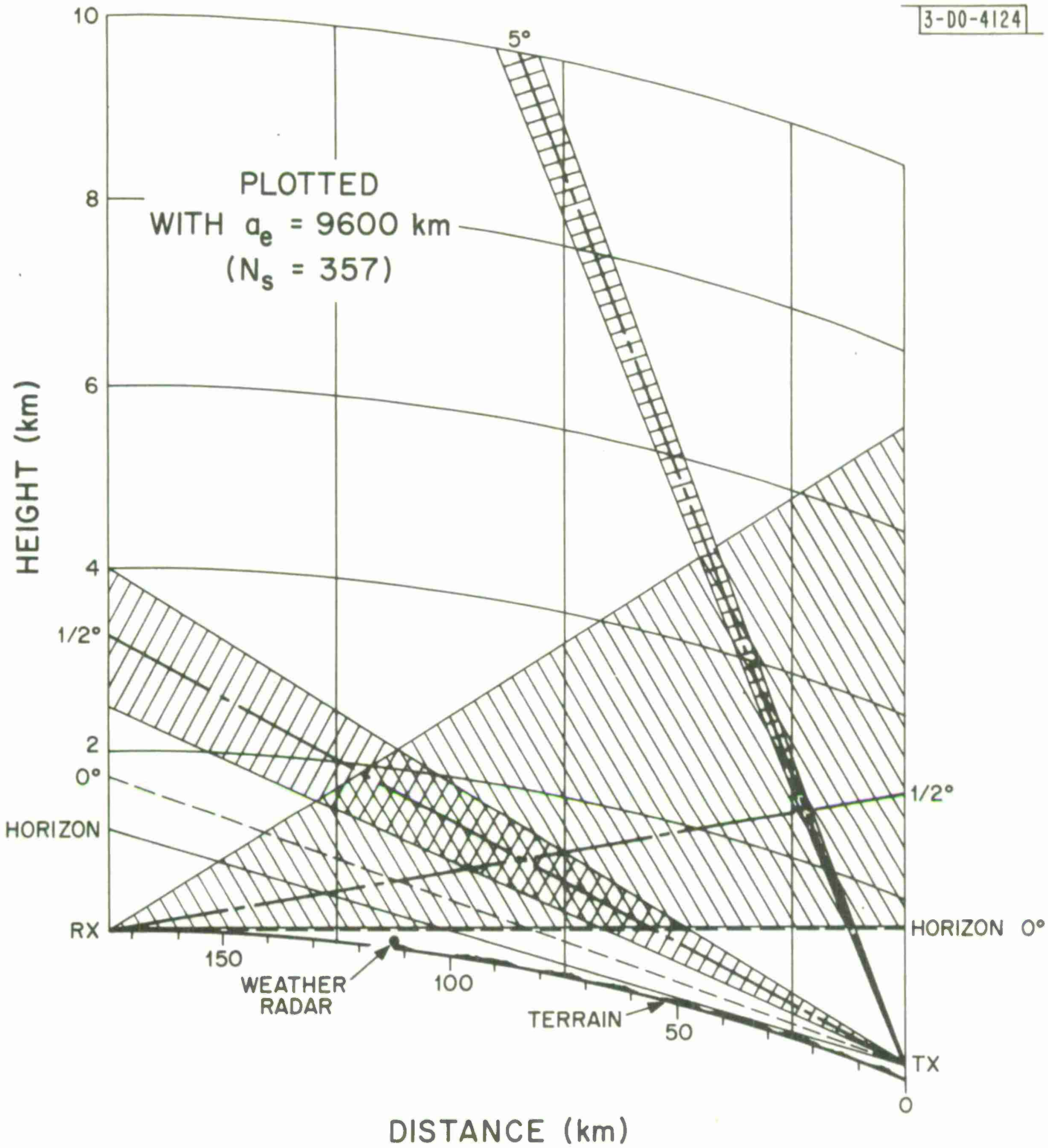

CROSS SECTION FOR SAMPLE PATH
HIGHLANDS, N. J. to WILDWOOD, N. J.

Fig. 3.

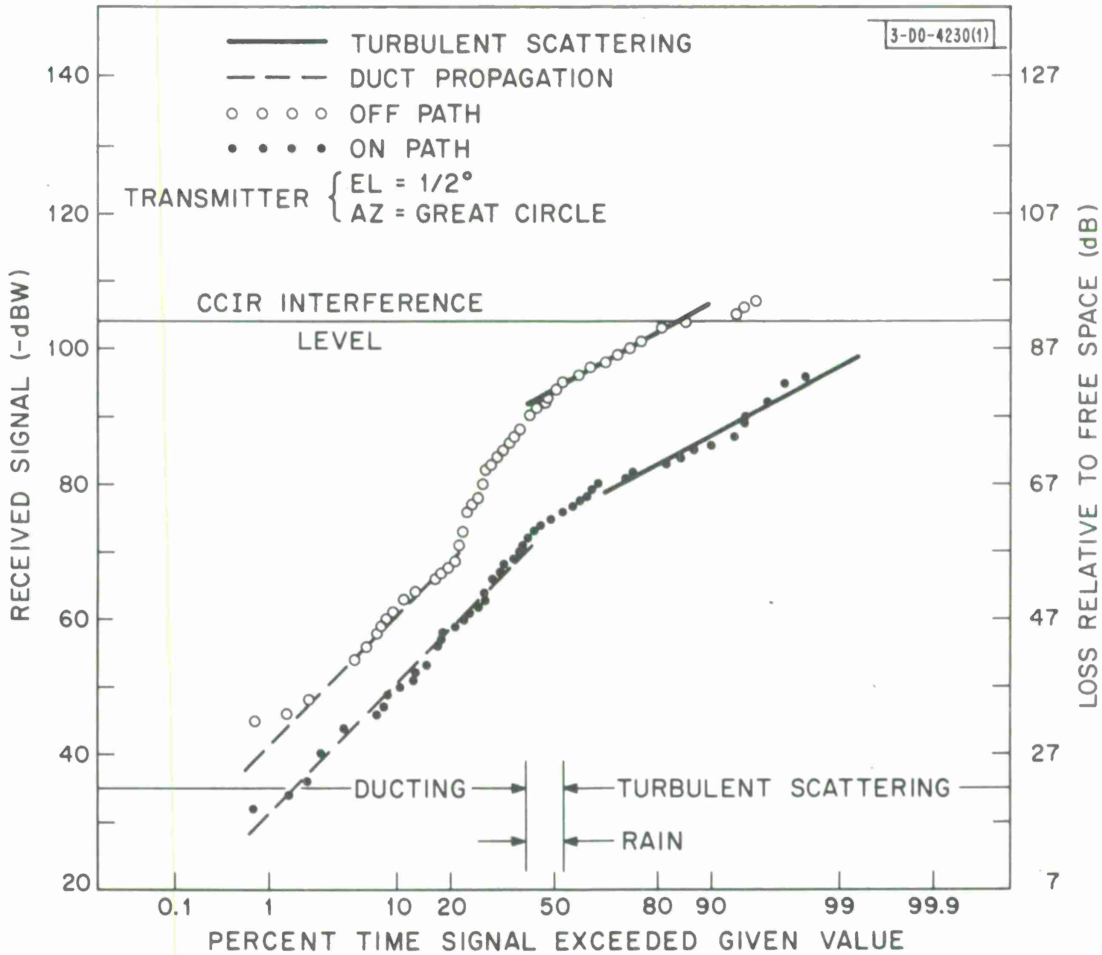

TROPOSCATTER DATA ON-PATH AND OFF-PATH
5-MINUTE MEDIAN SAMPLED ONE/HOUR
2-9 AUG 66 176.3-KM PATH HIGHLANDS TO WILDWOOD, N.J.

Fig. 4.

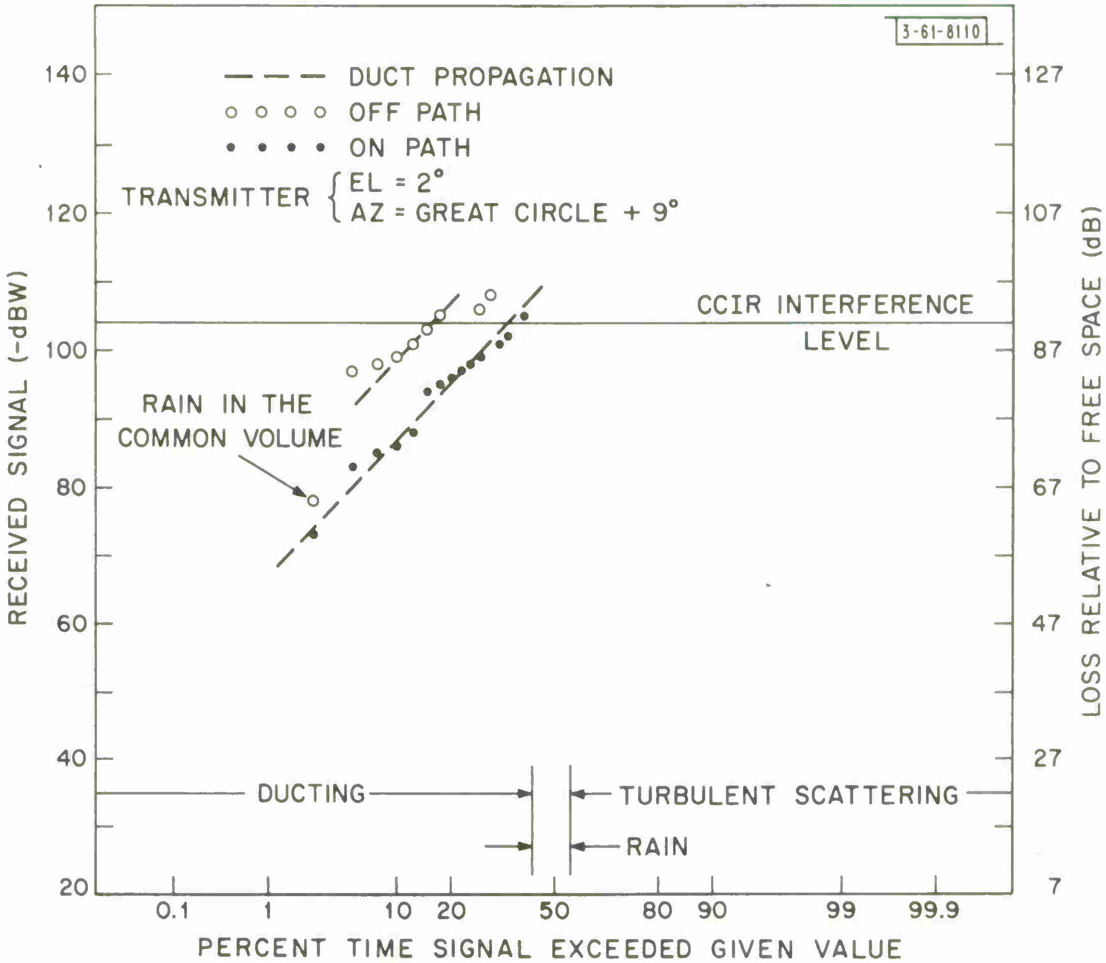

TROPOSCATTER DATA ON-PATH AND OFF-PATH
5-MINUTE MEDIAN SAMPLED ONE/THREE HOURS
2-9 AUG 66 176.3-KM PATH HIGHLANDS TO WILDWOOD, N.J.

Fig. 5.

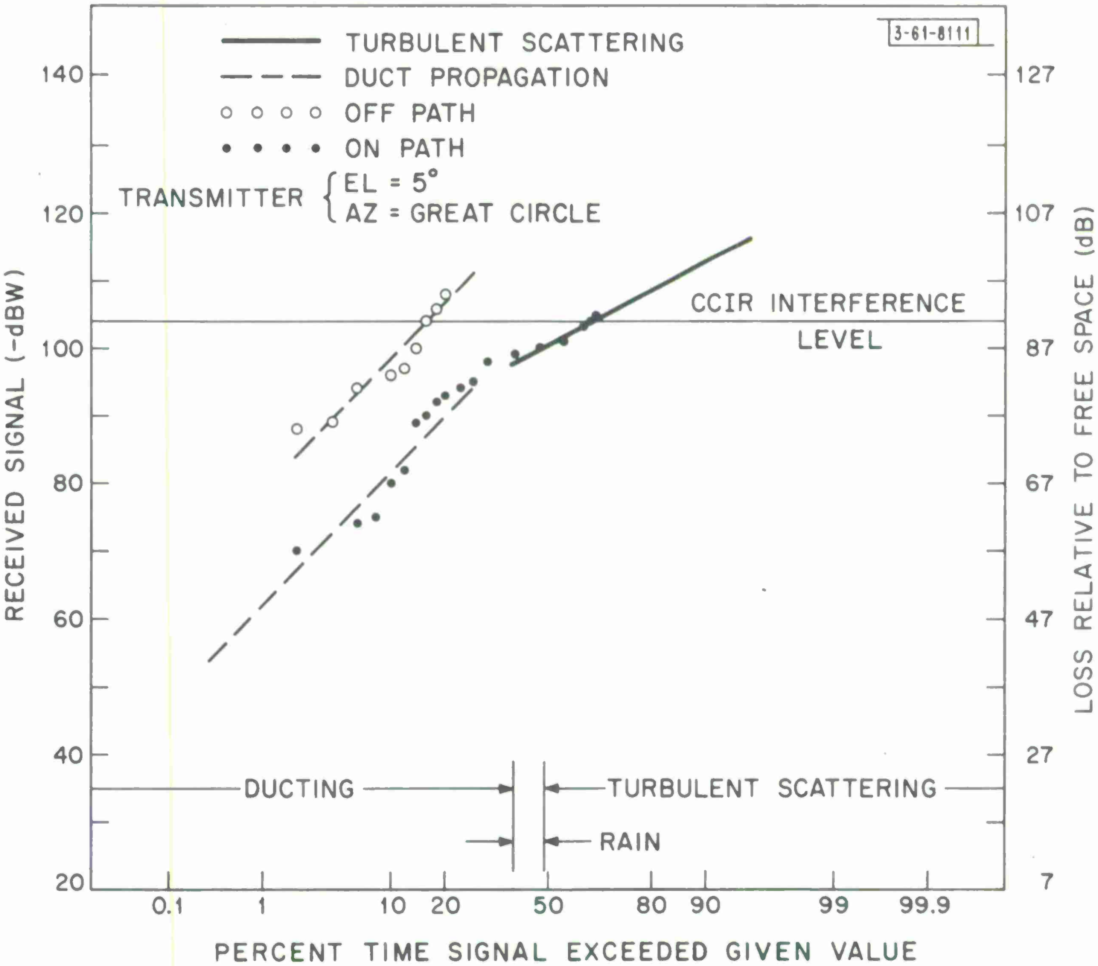

TROPOSCATTER DATA ON-PATH AND OFF-PATH
5-MINUTE MEDIAN SAMPLED ONE/THREE HOURS
2-9 AUG 66 176.3-KM PATH HIGHLANDS TO WILDWOOD, N.J.

Fig. 6.

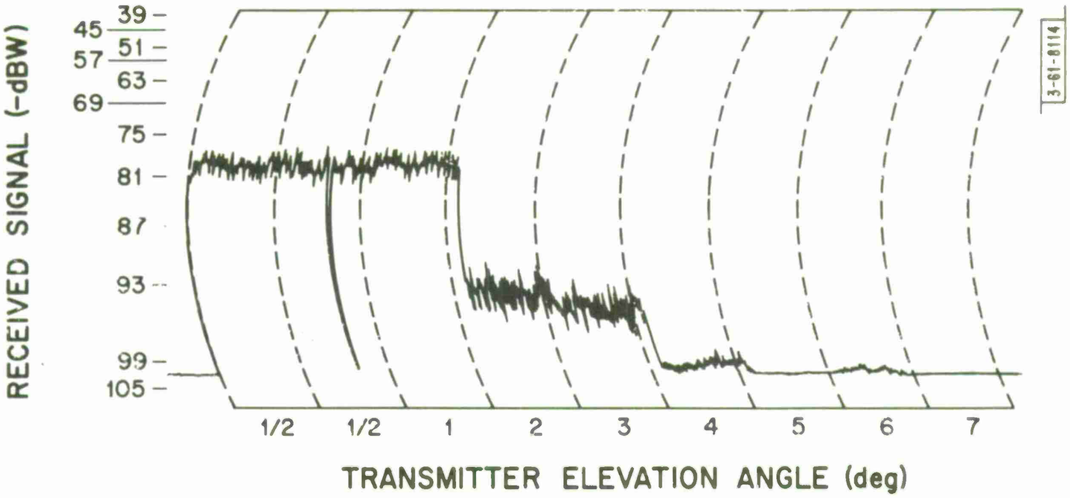

GREAT CIRCLE PATH
HIGHLANDS TO WILDWOOD, N. J. PATH
TURBULENT SCATTERING
3 AUG 66 1400 HR EST

Fig. 7.

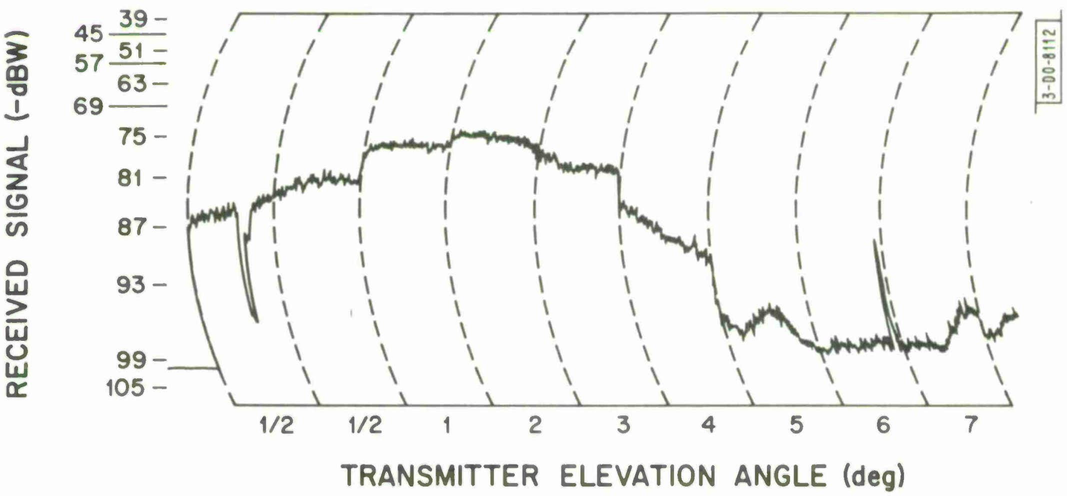

GREAT CIRCLE PATH
HIGHLANDS TO WILDWOOD, N. J. PATH
RAIN SCATTERING
2 AUG 66 2200 HR EST

Fig. 8.

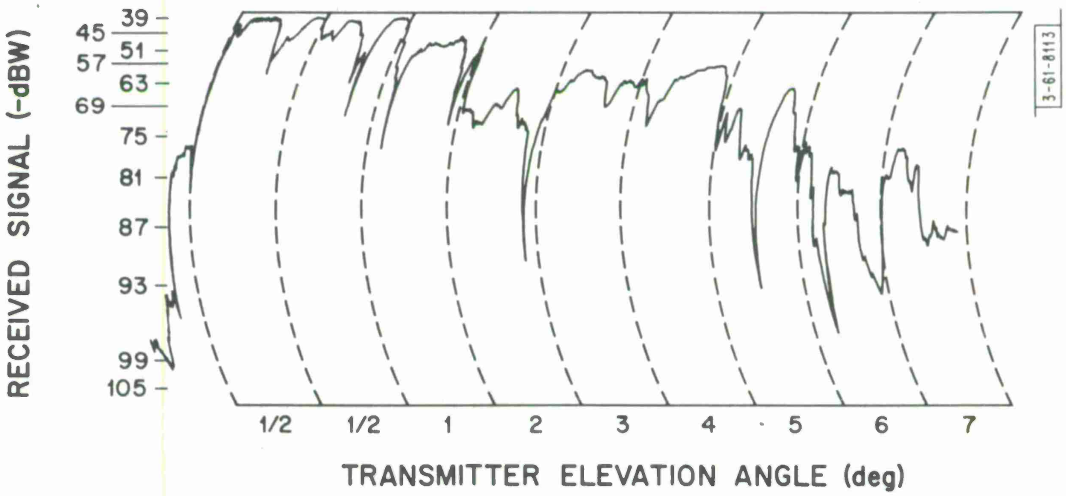

GREAT CIRCLE PATH
HIGHLANDS TO WILDWOOD, N. J. PATH
DUCTING CONDITIONS
4 AUG 66 0100 HR EST

Fig. 9.

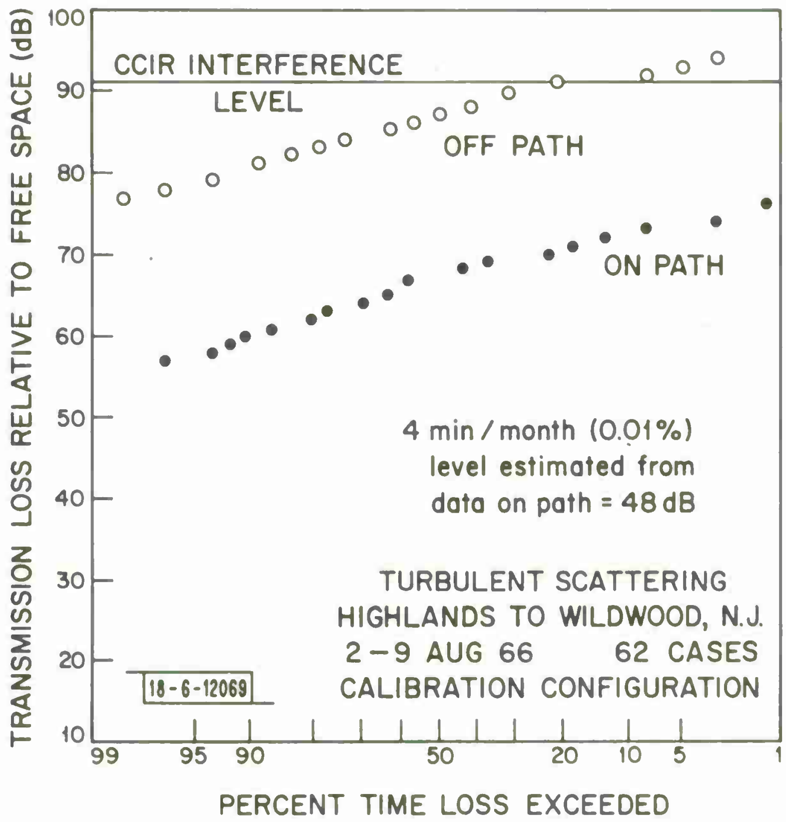

TRANSMISSION LOSS RELATIVE TO FREE SPACE (dB)
100
90
80
70
60
50
40
30
20
10
CCIR INTERFERENCE
LEVEL
OFF PATH
ON PATH
4 min / month (0.01%)
level estimated from
data on path = 48 dB
TURBULENT SCATTERING
HIGHLANDS TO WILDWOOD, N.J.
2 – 9 AUG 66 62 CASES
CALIBRATION CONFIGURATION
18-6-12069
99
95
90
50
20
10
5
1
PERCENT TIME LOSS EXCEEDED

Fig. 10.

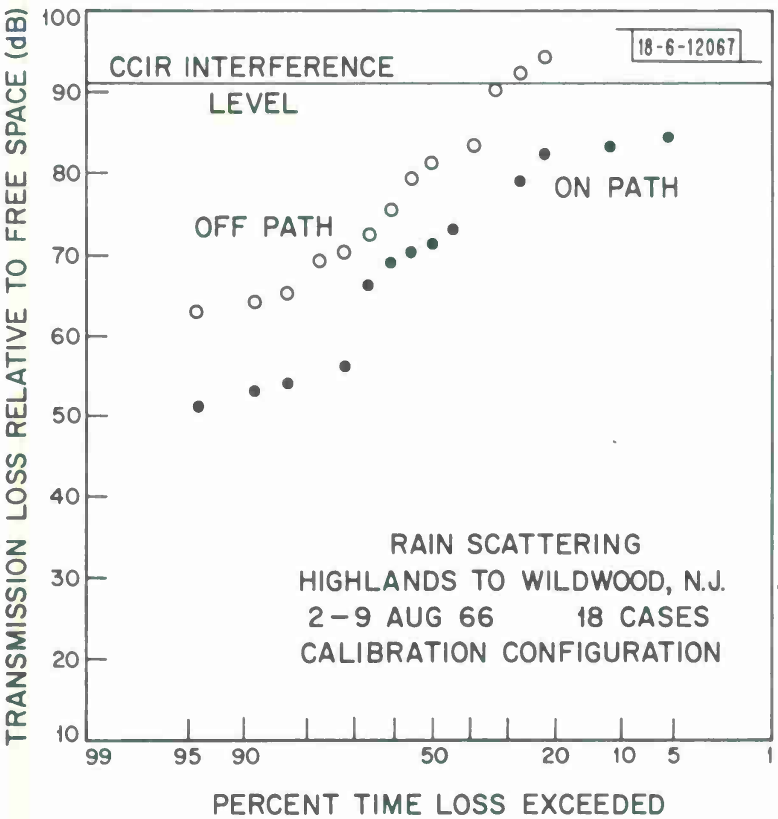

18-6-12067
CCIR INTERFERENCE
LEVEL
OFF PATH
ON PATH
RAIN SCATTERING
HIGHLANDS TO WILDWOOD, N.J.
2–9 AUG 66 18 CASES
CALIBRATION CONFIGURATION
TRANSMISSION LOSS RELATIVE TO FREE SPACE (dB)
PERCENT TIME LOSS EXCEEDED
100
90
80
70
60
50
40
30
20
10
99
95
90
50
20
10
5
1

Fig. 11.

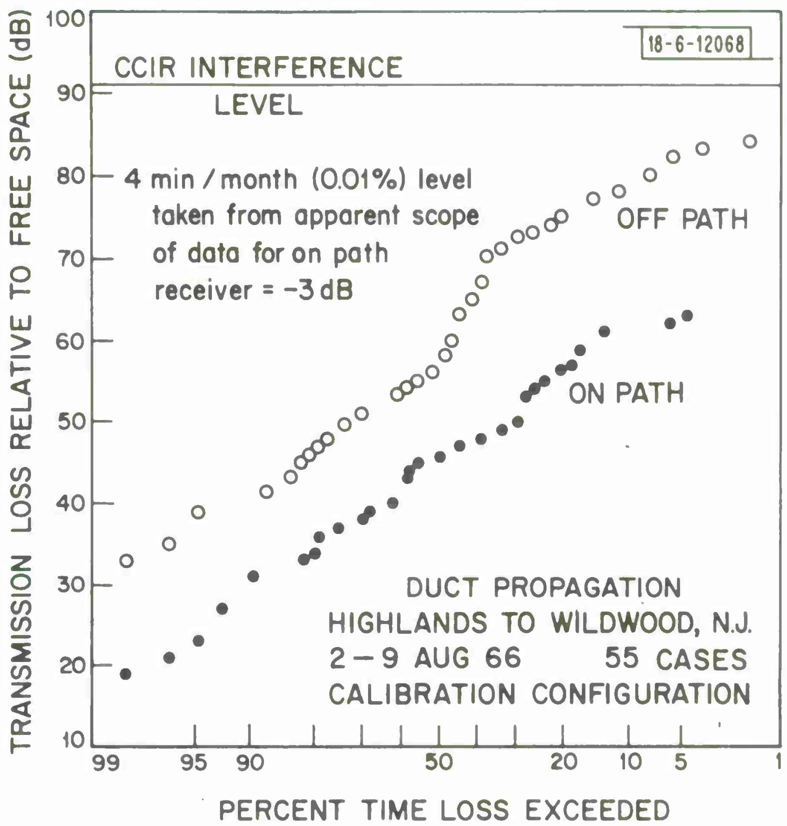

18-6-12068
CCIR INTERFERENCE
LEVEL
4 min / month (0.01%) level
taken from apparent scope
of data for on path
receiver = −3 dB
OFF PATH
ON PATH
DUCT PROPAGATION
HIGHLANDS TO WILDWOOD, N.J.
2 – 9 AUG 66
55 CASES
CALIBRATION CONFIGURATION
TRANSMISSION LOSS RELATIVE TO FREE SPACE (dB)
100
90
80
70
60
50
40
30
20
10
99
95
90
50
20
10
5
1
PERCENT TIME LOSS EXCEEDED

Fig. 12.

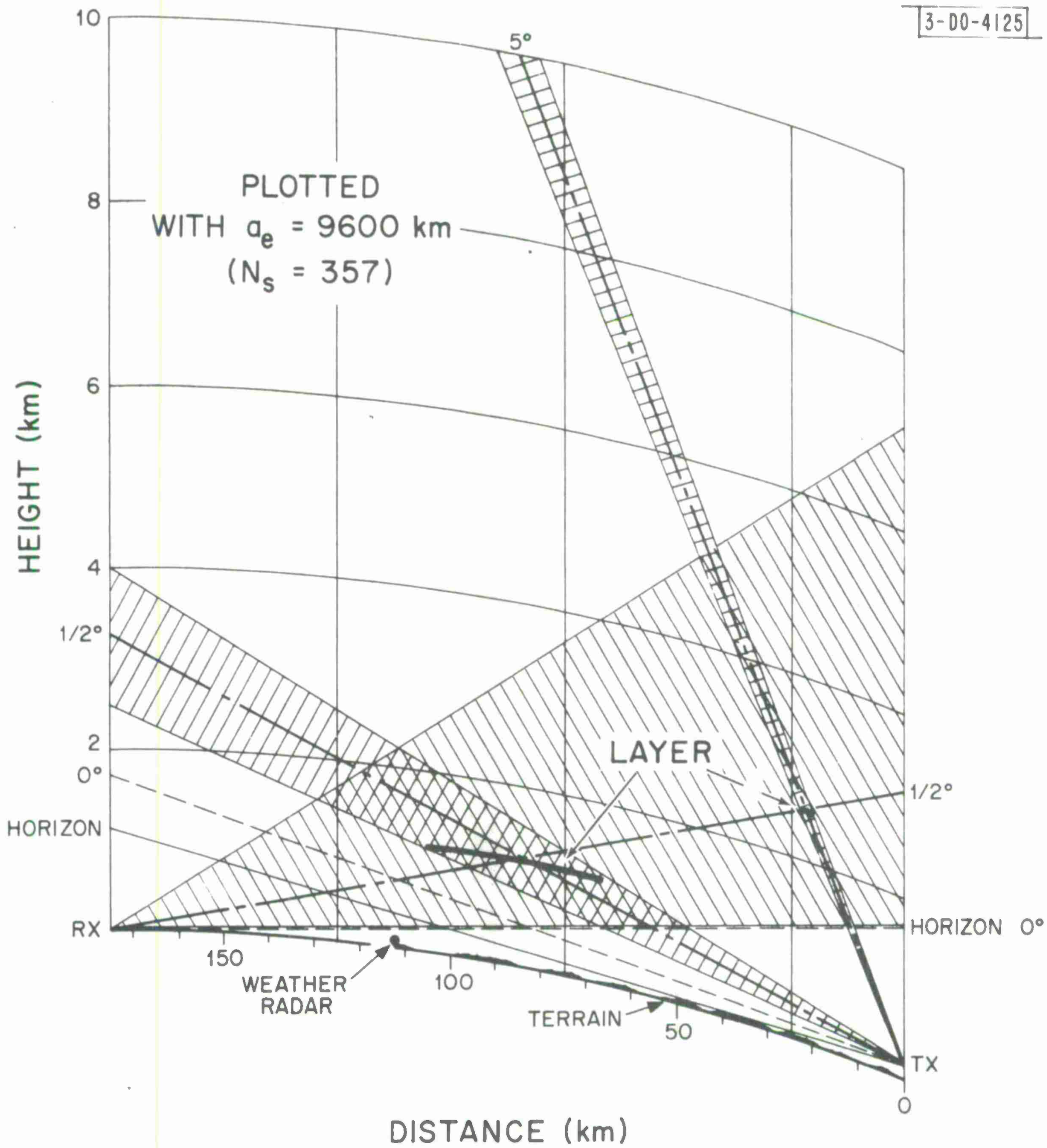

CROSS SECTION FOR TURBULENT LAYER SCATTERING

Fig. 13.

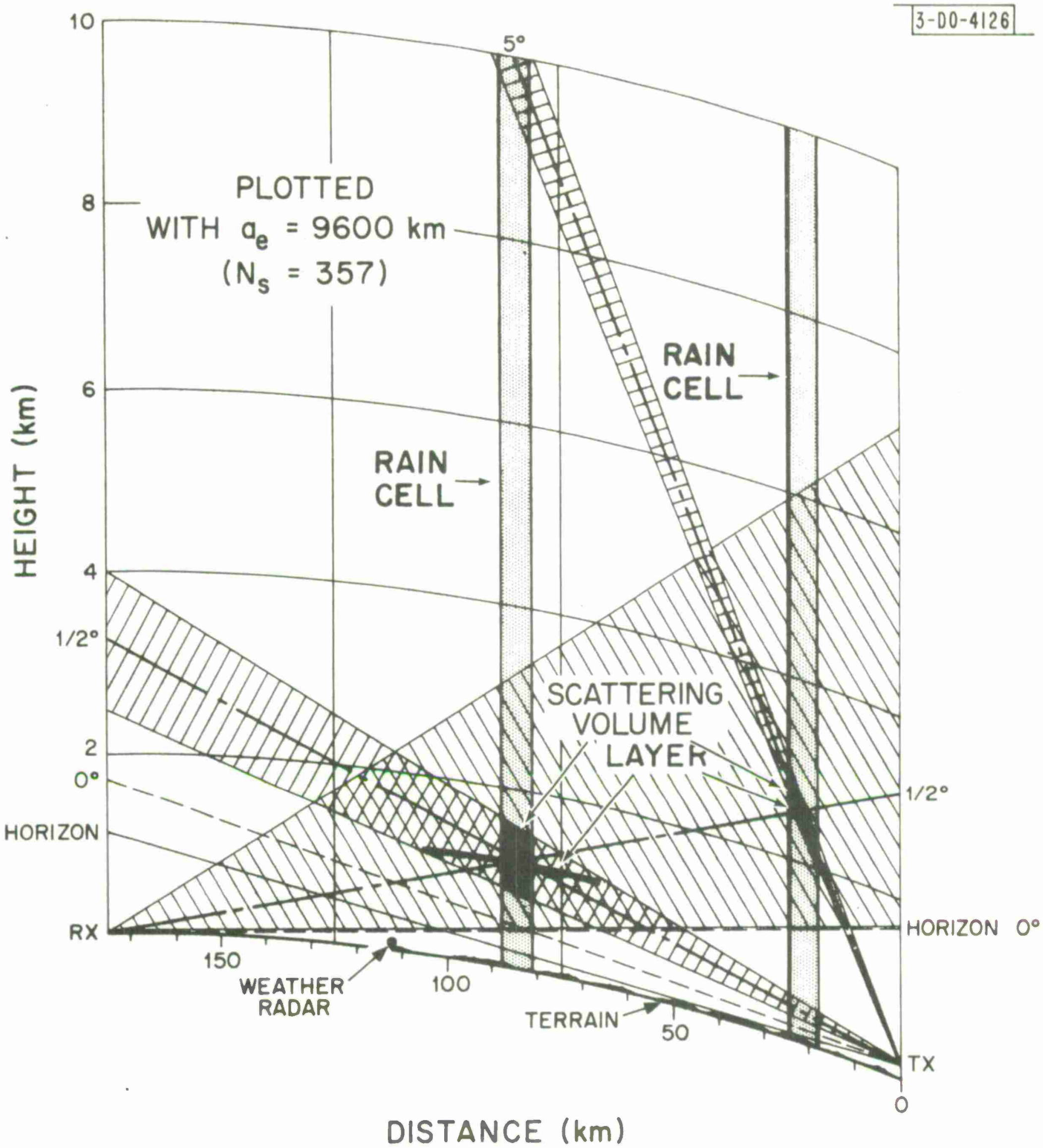

CROSS SECTION FOR PRECIPITATION SCATTERING

Fig. 14.

UNCLASSIFIED

Security Classification

DOCUMENT CONTROL DATA – R&D

(Security classification of title, body of abstract and indexing annotation must be entered when the overall report is classified)

1. ORIGINATING ACTIVITY *(Corporate author)* Lincoln Laboratory, M.I.T.	2a. REPORT SECURITY CLASSIFICATION Unclassified 2b. GROUP None

3. REPORT TITLE

Predictions of Transhorizon Field Strengths Using Modeling Techniques

4. DESCRIPTIVE NOTES *(Type of report and inclusive dates)*

Technical Note

5. AUTHOR(S) *(Last name, first name, initial)*

Crane, Robert K.

6. REPORT DATE	7a. TOTAL NO. OF PAGES	7b. NO. OF REFS
17 October 1969	32	14

8a. CONTRACT OR GRANT NO. AF 19(628)-5167 b. PROJECT NO. 649L c. d.	9a. ORIGINATOR'S REPORT NUMBER(S) Technical Note 1969-53 9b. OTHER REPORT NO(S) *(Any other numbers that may be assigned this report)* ESD-TR-69-320

10. AVAILABILITY/LIMITATION NOTICES

This document has been approved for public release and sale; its distribution is unlimited.

11. SUPPLEMENTARY NOTES	12. SPONSORING MILITARY ACTIVITY
None	Air Force Systems Command, USAF

13. ABSTRACT

Four propagation mechanisms are known which can cause detectable signal levels beyond the horizon. To investigate the potential of these mechanisms for causing interference, typical and extreme values were computed for models of the different propagation mechanisms, terrain diffraction, turbulent scattering, precipitation scattering, and ducting. The propagation path used for the model computations was 175 km long passing over irregular low lying terrain. The terminals of the path were taken to model a possible satellite earth station, radio relay station configuration. The radio relay station was assumed to have an antenna with a 2.5° half-power beamwidth pointing at an elevation angle of 0.5° to the horizon. The earth station antenna was assumed to have a 0.5° half-power beamwidth. A wavelength of 5 cm was used for the computations. Using the CCIR recommendations as a standard for interference levels, a propagation loss of less than 91 db relative to free space will cause interference for this path.

The highest signal strengths for this path were caused by turbulent scattering, precipitation scattering, and ducting. For both antennas elevated 0.5° to the horizon and pointed along the great circle route values of loss relative to free space of 50 db were computed for an extremely strong turbulent layer, 70 db for a typical turbulent layer and 58 db for a typical thundershower. For each of these computations the layer or storm was placed in the center of the common volume. For the antennas elevated to the same angle but each pointed approximately 7° off axis the extreme layer and the storm would cause interference, the computed loss for each being 80 and 58 db, respectively. For both antennas pointed along the great circle path and the earth station antenna at 5.0 elevation angle, precipitation scattering would cause interference with a loss of 69 db. For ducting and both antennas pointed along the great circle path and at elevations below 0.5, fields in excess of free space are possible.

The model computations show that for a spacing of 175 km, with low lying intervening terrain, and with the earth station antenna elevated above 5° precipitation scattering and ducting will be the only sources of interference. The problem of ducting can be reduced by siting so that shielding hills surround the earth station keeping the minimum elevation angle above 0.5.

14. KEY WORDS

transhorizon field strengths	space communications	ducting
modeling techniques	scattering	radio relay systems
propagation mechanisms	terrain diffraction	